Electric field effects on phase transitions in the 8CB liquid crystal doped with ferroelectric nanoparticles

Y. Lin*
Unité de Dynamique et Structure des Matériaux Moléculaires (UDSMM), Université du Littoral Côte d'Opale (ULCO), 62228 Calais, France

A. Daoudi and A. Segovia-Mera
Unité de Dynamique et Structure des Matériaux Moléculaires (UDSMM), Université du Littoral Côte d'Opale (ULCO), 59140 Dunkerque, France

F. Dubois, C. Legrand, and R. Douali
Unité de Dynamique et Structure des Matériaux Moléculaires (UDSMM), Université du Littoral Côte d'Opale (ULCO), 62228 Calais, France
(Received 8 March 2016; published 3 June 2016)

The influence of a low ac electric field on phase transitions is discussed in the case of a nematic liquid crystal 4-*n*-octyl-4′-cyanobiphenyl (8CB) doped with $Sn_2P_2S_6$ ferroelectric nanoparticles. The phase-transition temperatures obtained from temperature-dependent dielectric measurements were higher than those determined by the calorimetric method. This difference is explained by the presence of the measuring electric field which induces two effects. The first one is the amplification of the interactions between the nanoparticle polarization and the liquid-crystal order parameter. The second one is the field-induced disaggregation or aggregation process at high nanoparticle concentrations.

DOI: 10.1103/PhysRevE.93.062702

I. INTRODUCTION

In recent years, there has been a great deal of scientific interest in doping of liquid crystals with a small concentration of ferroelectric nanoparticles [1–5]. These nanocolloids present some higher performances than the pure liquid crystals, opening new perspectives for applications in many domains, including electronic and display [2,6,7], optical communications [8,9], and microwave applications [10,11]. For example, barium titanate ($BaTiO_3$) and tin-hypodiphosphate ($Sn_2P_2S_6$) ferroelectric nanoparticles coated with a surfactant (oleic acid) and dispersed in a nematic liquid crystal were reported to enhance optical birefringence [4], alter dielectric anisotropy [1–3], shift the phase-transition temperatures [12], and decrease the threshold voltage of the Fredericks transition [1]. When increasing nanoparticle concentration, the performance of the doped liquid crystal can be degraded due to aggregate formation. Otherwise, it has been shown that a low electric field can induce a separation of nanoparticles in aggregates [13]; this effect should also be observed in phase-transition temperatures.

In this work, we explore the idea that application of a low ac sinusoidal electric field on 4-*n*-octyl-4′-cyanobiphenyl (8CB) liquid crystal doped with $Sn_2P_2S_6$ ferroelectric nanoparticles has an effect on phase-transition temperatures. For this reason, we present a comparative study of phase-transition temperatures determined using two different methods: temperature-dependent dielectric measurements and differential scanning calorimetry (DSC).

II. MATERIALS AND EXPERIMENTAL SETUP

A. Materials and preparation of samples

As a host material, we used the 8CB liquid crystal (Frinton Laboratories, USA), which presents a large dielectric anisotropy $\Delta\varepsilon' = \varepsilon'_{\parallel} - \varepsilon'_{\perp} \approx 8$, where $\varepsilon'_{\parallel} \approx 13$ and $\varepsilon'_{\perp} \approx 5$ at room temperature, and it exhibits the following phase sequence: crystalline (C) –smectic-A (SmA) –nematic (N) –isotropic (I). We used $Sn_2P_2S_6$ ferroelectric nanoparticles elaborated by the Reznikov group. At room temperature, $Sn_2P_2S_6$ has a spontaneous polarization P of 14 $\mu C\,cm^{-2}$ parallel to the [101] direction of the monoclinic cell. The dielectric constant value depends on the structure of the sample, which varies from 300 for ceramic samples to 9000 for monodomain crystals.

As a first step, a dispersion of $Sn_2P_2S_6$ nanoparticles of 40 nm [14] in average diameter was prepared by milling large particles with oleic acid as a surfactant and heptane as a solvent in a vibration mill for 120 h. The resulting suspension presents a homogeneous dispersion of nanoparticles with a concentration of 0.1 wt. %. Doped liquid crystals were prepared with $Sn_2P_2S_6$ volume concentrations of $\phi_{NP} = 0.05\%$, 0.08%, 0.13%, 0.27%, and 0.54% by dissolving the initial suspension in the liquid crystal and mixing it with a magnetic stirrer. These doped liquid crystals were sonicated for a few hours, and the solvent was then slowly evaporated at $T = 50\,^{\circ}C$.

B. Experimental setup

The dispersion quality of ferroelectric particles in the liquid crystal was checked by an Olympus polarized optical microscope, which showed the appearance of a few big aggregates for high concentrations ($\phi_{NP} > 0.13\%$). Obviously, smaller and invisible aggregates can exist with all concentrations. These invisible aggregates can be considered as particles with dipolar moments.

Differential scanning calorimetry (DSC) measurements were performed on TA Instruments (DSCQ1000) equipped with a liquid nitrogen system allowing cooling and heating ramps. A rate of $2\,^{\circ}C/min$ (heating and cooling) was applied in the temperature range from 20 to $80\,^{\circ}C$.

For the dielectric measurements, we used commercial cells from PPW AWAT (Poland); they are made from two glass

*yaochen.lin@univ-littoral.fr

substrates coated with conducting ITO (indium tin oxide) layers having a resistance of 10 Ω/square. On ITO layers, a polymer is coated to align the liquid-crystal molecules with one of the following two configurations: planar orientation when the molecules are parallel to the glass plan, and homeotropic orientation when they are perpendicular. In the first case, the measuring electric field is perpendicular to the long molecular axis and the measured dielectric constant is denoted as $\varepsilon_\perp$; in the second case, the dielectric constant is denoted as $\varepsilon_\parallel$. The dielectric measuring cells have a thickness of 20 μm and were filled with the nanocolloids by the capillary effect. The temperature of the sample is ensured by a mechanical cell designed in the laboratory; it contains heating resistors and a Pt100 temperature sensor. A Eurotherm 3504 controller allows an accuracy of 0.02 °C. The electrical contact was made with SMA coaxial connectors deposited on the ITO layers.

Dielectric measurements were made using a Hewlett Packard 4284*A* impedance analyzer covering the frequency range from $f = 20$ Hz to 1 MHz. The amplitude of the measuring sinusoidal electric field was fixed at 0.1 V. Assuming that C_o is the empty cell capacitance, the real and imaginary parts of the complex dielectric permittivity ε^* ($\varepsilon^* = \varepsilon' - j\varepsilon''$) can be expressed from measured capacitance C and conductance G of the filled cell using the following relations:

$$\varepsilon'(f) = \frac{C(f)}{C_o}, \tag{1}$$

$$\varepsilon''(f) = \frac{G(f)}{2\pi f C_o}. \tag{2}$$

The cell temperature T varies between 30 and 42 °C with a step of 0.05 °C. Each temperature is stabilized during 400 s before dielectric data acquisition.

To estimate the statistical measuring errors in comparison with any variation due to the effect of nanoparticles, we prepared a minimum of two mixtures for each concentration of nanoparticles, and different samples have been characterized. For each mixture, DSC measurements have been done for at least two samples, and each sample has been measured two times in the same conditions. In the dielectric measurements and for each orientation, a minimum of two samples have been measured for each mixture.

III. RESULTS AND DISCUSSION

A. Temperature dependence of static permittivity and phase transitions

Figure 1 shows examples of dielectric spectra obtained in two orientations for the pure and the doped liquid crystal ($\phi_{\rm NP} = 0.54\%$). In $\varepsilon'_\parallel(f)$ plots [Fig. 1(a)], three parts can be distinguished: at low frequencies ($f < 100$ Hz), $\varepsilon'_\parallel$ increases when frequency decreases; this effect is attributed to the accumulation of ionic charges near electrodes (electrode polarization effect). The unchanged measured value between 500 Hz and 100 kHz corresponds to the static dielectric constant $\varepsilon'_{s\parallel}$. For $f > 100$ kHz, the spectra show the beginning of a dielectric relaxation process that corresponds to the well-known dipolar relaxation mechanism associated with rotation of the liquid-crystal molecules around their short axis [15]. In planar orientation, the dielectric spectra [Fig. 1(b)]

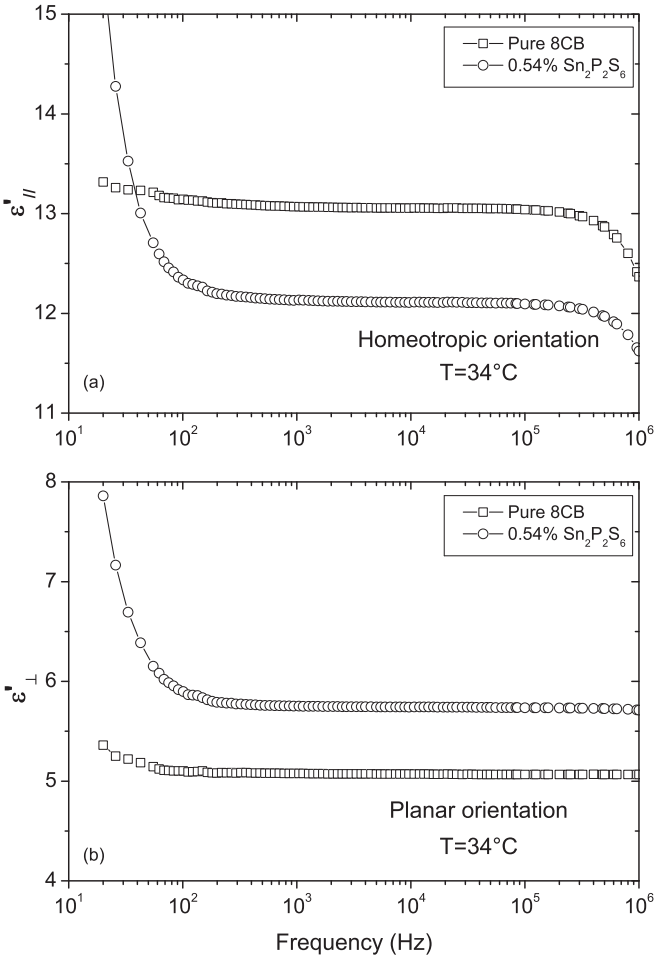

FIG. 1. Dielectric spectra of the pure 8CB and 8CB/$Sn_2P_2S_6$ nanocolloid with a volume fraction $\phi_{\rm NP} = 0.54\%$ for (a) homeotropic and (b) planar orientations.

evidence the electrode polarization effect at the low-frequency domain (up to 100 Hz) and static dielectric constant $\varepsilon'_{s\perp}$ (beyond 500 Hz). We focus our discussion below only on the temperature dependence of the static dielectric permittivities denoted as $\varepsilon'_\parallel$ and $\varepsilon'_\perp$.

Dielectric measurements versus temperature show smectic-*A*–nematic and nematic-isotropic phase transitions. An example is given in Fig. 2 for the doped liquid crystal with $\phi_{\rm NP} = 0.08\%$. The $\varepsilon'_\parallel(T)$ plot obtained in the homeotropic orientation shows a maximum at the smectic-*A*–nematic phase-transition temperature $T_{{\rm Sm}A\text{-}N}$ [Fig. 2(a)]. In the planar orientation, the $\varepsilon'_\perp(T)$ plot presents an inflection point at $T_{{\rm Sm}A\text{-}N}$ [Fig. 2(b)]; the same behavior was also reported from measurements of refraction index anisotropy Δn [16]. Both $\varepsilon'_\parallel(T)$ and $\varepsilon'_\perp(T)$ plots show a discontinuous change at the phase-transition temperature $T_{N\text{-}I}$, revealing the first-order nature of this transition. Let us notice that the values of $T_{{\rm Sm}A\text{-}N}$ and $T_{N\text{-}I}$ obtained from the planar orientation are the same as those determined for the homeotropic orientation. For this reason, in this section we only use data from the planar orientation. To determine more accurately the phase-transition temperatures, we present in Fig. 3 the derivative of $\varepsilon'_\perp$ with respect to temperature as a function of temperature.

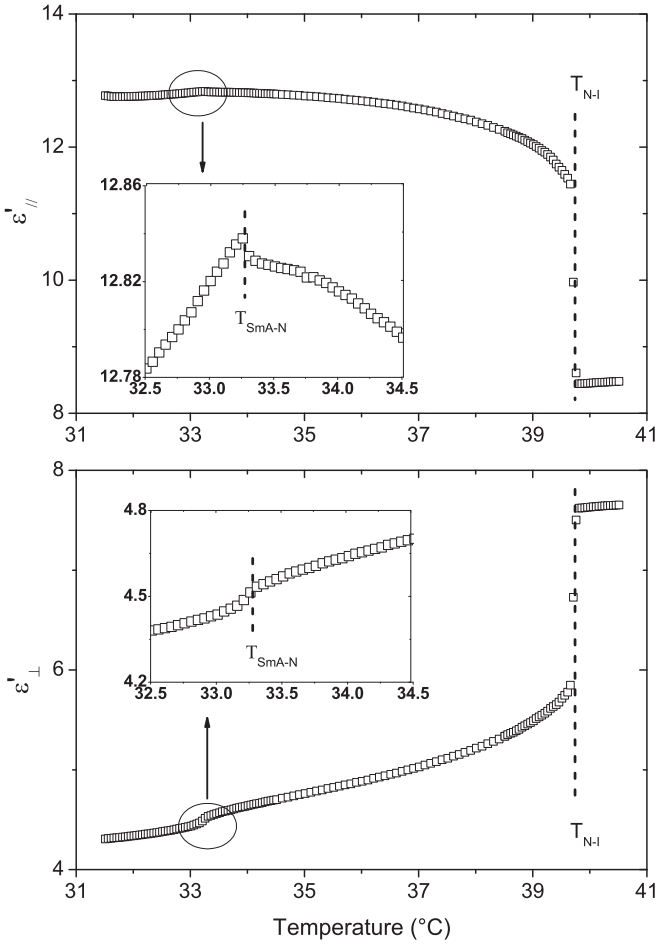

FIG. 2. Temperature-dependent (a) $\varepsilon'_{\parallel}$ and (b) $\varepsilon'_{\perp}$ of the doped liquid crystal ($\phi_{\mathrm{NP}} = 0.08\%$). Insets: enlarged regions of the smectic-A–nematic phase transition.

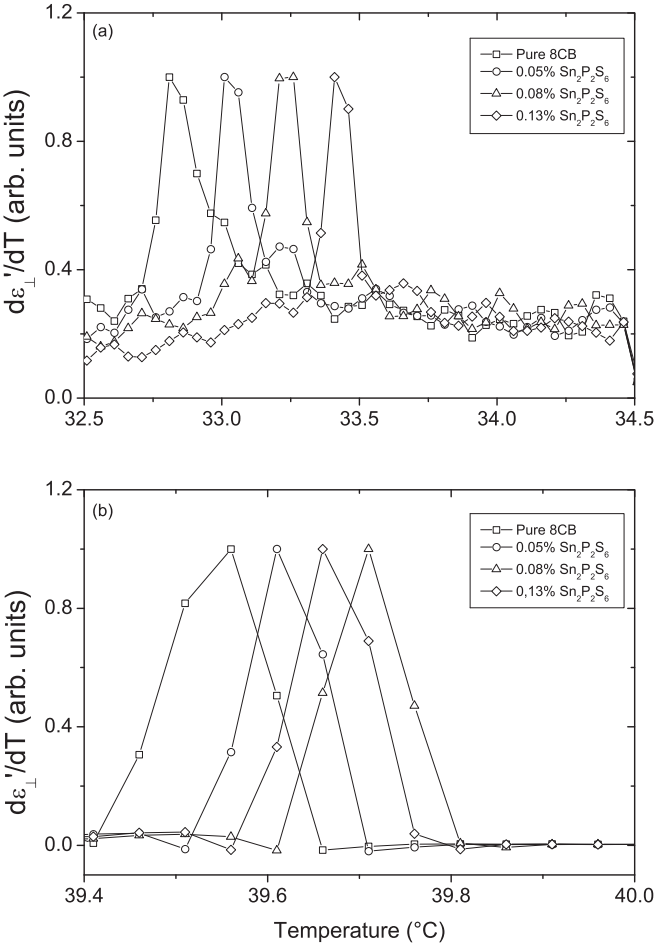

FIG. 3. The derivative of $\varepsilon'_{\perp}$ obtained from the planar orientation as a function of temperature for the pure liquid crystal and nanocolloids: (a) smectic-A–nematic and (b) nematic-isotropic phase transition regions.

The phase-transition temperature values obtained from dielectric measurements are given in Table I(a). For comparison, we reported in Table I(b) the phase-transition temperature values determined by DSC measurements already published in our previous paper [14]. We remind the reader below of the main results of the DSC study.

B. Phase-transition temperatures from DSC characterization

$\Delta T_{N\text{-}I}$ and $\Delta T_{\mathrm{Sm}A\text{-}N}$ in Table I(b) correspond to the observed shifts of phase-transition temperatures between the pure 8CB and 8CB/$Sn_2P_2S_6$ nanocolloids. As discussed previously [14], the shifts $\Delta T_{N\text{-}I}$ and $\Delta T_{\mathrm{Sm}A\text{-}N}$ result from a competition between two principal effects: the first effect is related to the nanoparticles' permanent polarization and is favorable to the increase of phase-transition temperatures. The second effect, which affects phase transitions, is related to the anchoring interactions between liquid-crystal molecules and inclusions, which were reported for different kinds of inclusions [17,18]. These interactions are unfavorable to the increase of phase-transition temperatures because they decrease the liquid-crystal order parameter. Due to the anchoring interactions, increasing nanoparticle concentration induces decreases of the nematic-isotropic and smectic-A–nematic phase-transition temperatures [19–21]. In the case of strong polar interactions between nanoparticles and liquid-crystal molecules, as, e.g., for our 8CB/$Sn_2P_2S_6$ system [14], the increase of $T_{N\text{-}I}$ linked to the polarization effect has been theoretically evaluated by Lopatina [12]. It is given by the following expression:

$$\Delta T_{N\text{-}I} = 1.03\frac{\phi_{\mathrm{NP}}\Delta\varepsilon P^2}{135k_B\rho_{\mathrm{LC}}\varepsilon_0\varepsilon^2}, \tag{3}$$

where $\Delta\varepsilon, k_B, \rho_{\mathrm{LC}}, \varepsilon_0$, and $\varepsilon = (2\varepsilon_{\perp} + \varepsilon_{\parallel})/3$ correspond to the liquid-crystal anisotropy, the Boltzmann constant, the liquid-crystal molecular density, the permittivity of free space, and the average dielectric permittivity, respectively. On the other hand, the decrease of $T_{N\text{-}I}$ linked to the anchoring interactions can be estimated using the simplest version of the Matsuyama model [19,20]:

$$\Delta T_{N\text{-}I} = -\phi_{\mathrm{NP}}T^0_{N\text{-}I}, \tag{4}$$

where $T^0_{N\text{-}I}$ represents $T_{N\text{-}I}$ of the pure liquid crystal. This simple equation expresses the so-called dilution effect. Using Eqs. (3) and (4) and the 8CB/$Sn_2P_2S_6$ parameters, we showed that the dilution effect is predominant and the global shift $\Delta T_{N\text{-}I}$ corresponds to a linear decrease versus the

TABLE I. Transition temperature shifts obtained from (a) dielectric measurements and (b) DSC.

				(a)		
ϕ_{NP} (%)	0	0.05	0.08	0.13	0.27	0.54
$T_{SmA\text{-}N}$ (°C)	**32.80**					
$\Delta T_{SmA\text{-}N}$	0	+0.20 (±0.02)	+0.45 (±0.04)	+0.60 (±0.04)	+0.75 (±0.05)	−0.10 (±0.08)
$T_{N\text{-}I}$ (°C)	**39.60**					
$\Delta T_{N\text{-}I}$	0	+0.05 (±0.03)	+0.15 (±0.03)	+0.10 (±0.05)	−0.25 (±0.05)	−2.50 (±0.08)
				(b)		
$T_{SmA\text{-}N}$ (°C)	**32.60**					
$\Delta T_{SmA\text{-}N}$	0	+0.05 (±0.01)	+0.10 (±0.01)	+0.20 (±0.01)	+0.40 (±0.02)	−0.50 (±0.02)
$T_{N\text{-}I}$ (°C)	**39.60**					
$\Delta T_{N\text{-}I}$	0	−0.30 (±0.01)	−0.40 (±0.01)	−0.60 (±0.01)	−1 (±0.01)	−3.30 (±0.02)

nanoparticles concentration. As discussed in our previous paper, the anchoring effect in $8CB/Sn_2P_2S_6$ nanocolloids is stronger than a simple dilution effect; this explains the difference between the observed $T_{N\text{-}I}$ decrease and the one estimated from Eqs. (3) and (4). For high concentrations, the polarization effect is reduced due to aggregate formation; thus the decrease of $T_{N\text{-}I}$ is more pronounced. Due to the stronger polarization effect near the smectic-*A*–nematic phase transition, $T_{SmA\text{-}N}$ can increase at low concentrations.

C. Comparison of phase-transition temperatures from DSC and dielectric measurements

From Table I and Fig. 4, we notice that the values of the phase-transition temperatures obtained from dielectric measurements are higher than those determined by DSC. This means that the liquid-crystal order parameter S_{LC} is higher for samples studied by dielectric measurements. This difference can be explained by the two different sample configurations used in DSC and dielectric measurements. The DSC measurements are carried out on free drop samples submitted only to thermal treatments, whereas the temperature-dependent dielectric characterizations are performed on samples under an electric field in polymer-coated capacitive cells. The ordering of the liquid-crystal molecules in the capacitive cell without electric field should be better than that obtained in a free drop used in DSC measurements. In the case of a free drop, the long-range orientational order inside the volume is characterized by a distance of the order of 0.1 μm [22]. As shown in previous works, at a liquid-crystal–air interface, the molecules are oriented either along the surface normal, perpendicular to it, or tilted, depending on the type of liquid crystal [23]. Consequently, in the whole volume of a free drop, the orientation is not unidirectional; the total order parameter shown by the entire sample is slightly different from that of a unidimensional oriented sample [24,25]. In a capacitive cell used in our study, the liquid-crystal–air surface is very small compared to the whole sample; the orientation can be considered unidirectional due to the interactions between the liquid-crystal molecules and the aligning polymer layer coated on the ITO substrate [26]. Thus, S_{LC} and the corresponding phase-transition temperatures of the pure liquid crystal could be higher than those in a free drop sample. These increases can be amplified by applying a sufficiently strong electric field. Such an effect has been reported for an applied electric field strength of about 10^4 V/cm [27–29]. In our case, the measuring electric field is 50 V/cm; this value is too small to affect S_{LC}.

As shown in Table I, $T_{N\text{-}I}$ values of the pure liquid crystal obtained from DSC and dielectric measurements are similar; both methods also lead to close values of $T_{SmA\text{-}N}$. Thus, the liquid-crystal molecules and polymer interactions and the measuring electric field do not affect significantly S_{LC} of the pure liquid crystal.

In the case of nanocolloids, the nanoparticles are homogeneously dispersed in the whole volume. Their quantity at the substrate/liquid-crystal interface is too small to affect the surface interactions between polymer and liquid-crystal molecules in the capacitive cell; the orientation of liquid-crystal molecules should be the same for the nanocolloids as for the pure liquid crystal. For this reason, the higher phase-transition temperatures of nanocolloids observed during dielectric measurements cannot be explained by the capacitive cell configuration; it could, however, be linked to the measuring electric field. To explain this, it is important to understand the nanoparticle behavior in the presence of an ac electric field. This behavior has been studied by Evans [13]; we report here some of the principal conclusions of this study in relation to our experimental results.

First of all, we distinguish two kinds of inclusions in nanocolloids: single-dipole nanoparticles and aggregates with small or large dipole moments; to illustrate this, we present in Fig. 5 two single nanoparticles with different dipolar moment and two different kinds of aggregates resulting from the association of two and three single nanoparticles, respectively.

Without electric field, the two kinds of inclusions contribute to the polarization and anchoring effects, which lead to the phase-transition temperatures obtained by DSC (at $t = 0$ in Fig. 5) [14]. Due to the coupling between the liquid-crystal molecules and nanoparticles, the order parameters of nanoparticles S_{NP} and liquid crystal S_{LC} are related by the following equation developed by Lopatina [12]:

$$S_{NP} = 1 - \frac{k_B T}{K_{NP} S_{LC}}, \tag{5}$$

where K_{NP} describes the strength of the interactions. Let us notice that Eq. (5) is valid only for the case of strong interactions between S_{NP} and S_{LC}, which is the case for $8CB/Sn_2P_2S_6$ nanocolloids [14].

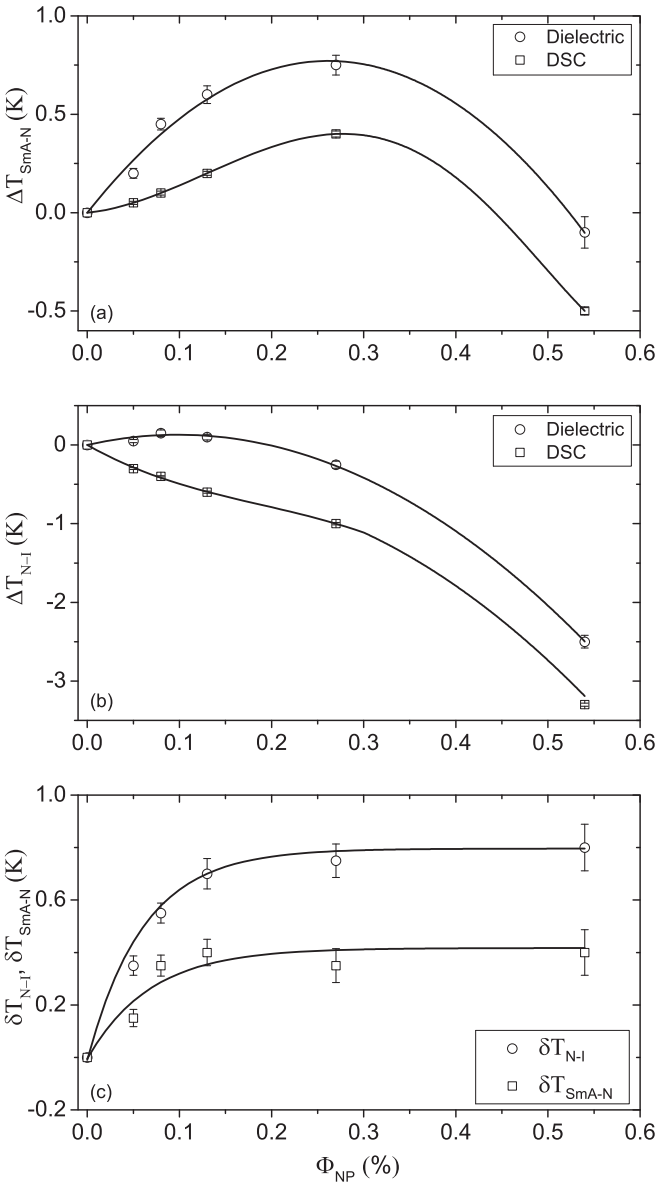

FIG. 4. (a) Shifts of smectic-A–nematic phase-transition temperatures induced by the nanoparticles; (b) shifts of nematic-isotropic phase-transition temperatures induced by the nanoparticles. (c) Differences between the shifts of phase-transition temperatures observed from DSC and temperature-dependent dielectric measurements: $\delta T = \Delta T_{\text{dielectric}} - \Delta T_{\text{DSC}}$. The lines are a guide to the eye. For some plots, the error bars are not visible due to the scales (see Table I).

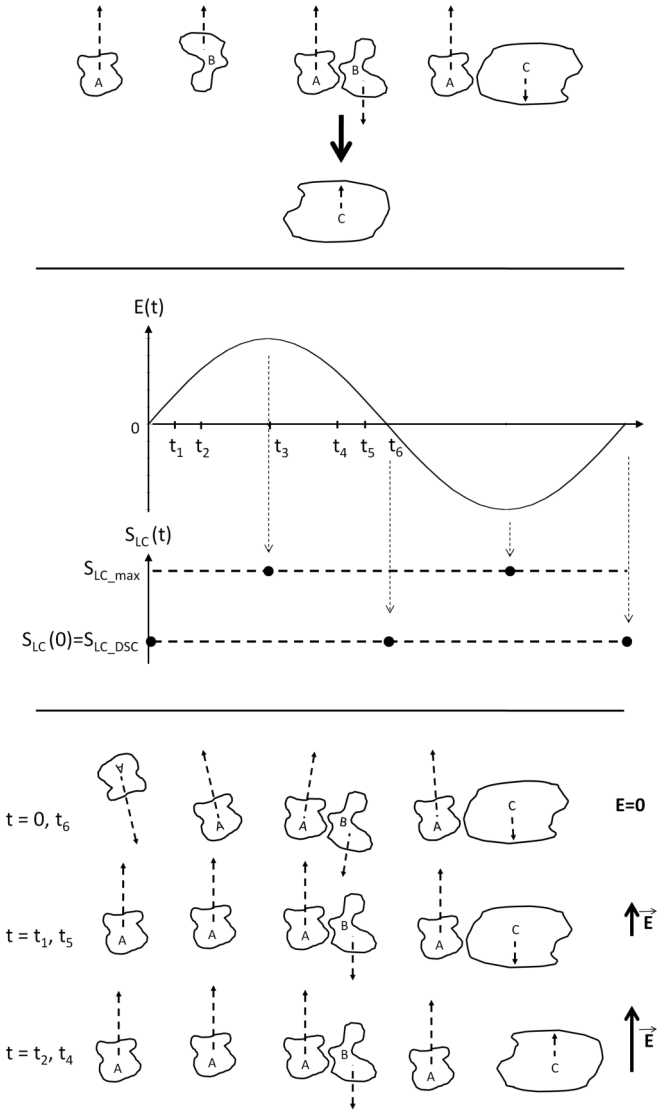

FIG. 5. Schematic illustration of a sinusoidal electric field effect on the order parameter of doped nematic liquid crystal. Top: examples of single-dipole nanoparticles and of corresponding aggregates ($p_A > p_B > p_C$). Middle: time-dependent sinusoidal electric field and corresponding optimal values of the order parameter. Bottom: orientation and disaggregation process of nanoparticles in the doped liquid crystal.

During the increasing step of the sinusoidal measuring electric field, two phenomena appear:

(i) The dipoles p (of single nanoparticles or aggregates) tend to align in the direction of the electric field, as shown at t_1 in Fig. 5; the polar order of nanoparticles improves S_{NP} and S_{LC} in accordance with Eq. (5).

(ii) Due to Coulomb interactions, the dipoles of nanoparticles tend to have an antiparallel arrangement forming an aggregate [30]. Despite these interactions, the contact between nanoparticles is not direct due to the oleic acid coating on nanoparticle surfaces. In such a situation, the separation of nanoparticles in an aggregate can be achieved by a relatively weak electric field, as evidenced by Evans [13]. Let us notice that for a given electric field, the disaggregation appears only for some aggregates where the coupling between the electric field and the dipole moments is predominant compared to the temperature influence ($k_B T$) and to the dipole-dipole interactions. In the case of an aggregate formed by two single-dipole nanoparticles, due to the strong electric field at the surface of a ferroelectric nanoparticle ($E \sim 10^{10}$ V/m), the measuring electric field used during dielectric measurements is not enough to induce the disaggregation. However, this aggregate acts as a new particle with a smaller dipole moment that induces a weaker electric field. When this new particle interacts with other particles (single or aggregates), they form a bigger aggregate with weaker interactions; thus, it is easier to

break them apart. Consequently, during the increasing step of the measuring electric field, the disaggregation process starts with the biggest aggregates when the electric field reaches a value sufficiently high; the disaggregation process is amplified when the electric field increases.

After the disaggregation, the separated particle dipoles (single-dipole or aggregates) align together in the same direction parallel to the electric field (at t_2 in Fig. 5); this amplifies the increase of S_{NP} and S_{LC}, as discussed above. At the maximum value of the ac electric field (at t_3 in Fig. 5), the polarization effect is predominant compared to the anchoring effects, and the order parameter reaches its maximum value $S_{\mathrm{LC\_max}}$ (Fig. 5).

During the decreasing step of the sinusoidal electric field, the aggregates reform. As the voltage approaches zero, the liquid crystal reaches its initial order parameter (at t_6 in Fig. 5).

When the measuring signal varies with time, it leads to a time-dependent order parameter $S_{\mathrm{LC}}(t)$; thus, the measured dielectric constant corresponds to the average value $\bar{S}_{\mathrm{LC}}$. From Fig. 5, we can clearly see that $\bar{S}_{\mathrm{LC}} > S_{\mathrm{LC\_DSC}}$, which explains the higher phase-transition temperatures determined from dielectric measurements. Let us notice that this increase can result from the alignment phenomenon only when the electric field is low or from both effects (alignment and disaggregation) when E is sufficiently high.

We plotted the concentration dependence of δT, which is the difference between the shifts obtained from dielectric measurements and those determined by DSC: $\delta T = \Delta T_{\mathrm{dielectric}} - \Delta T_{\mathrm{DSC}}$ [Fig. 4(c)]. From this figure, we can notice the following:

(a) The nanoparticle concentration dependencies of $\delta T_{N\text{-}I}$ and $\delta T_{\mathrm{Sm}A\text{-}N}$ are similar; the two plots show a quasilinear increase for low concentrations, and then the slopes decrease progressively at high concentrations. For low concentrations ($\phi_{\mathrm{NP}} \leqslant 0.13\%$), the nanoparticle dispersion is homogeneous (without aggregates); increasing the single-dipole nanoparticle quantity leads to an amplification of the polarization effect discussed above [point (i)]; thus, the order parameter and the phase-transition temperature increase. If the concentration increases more ($\phi_{\mathrm{NP}} > 0.13\%$), the distance between single-dipole nanoparticles decreases and the dipole-dipole interactions become stronger, thus aggregates are formed; the decrease of the single-dipole nanoparticle quantity is unfavorable for increasing the order parameter under electric field. On the other hand, this decrease of the single-dipole nanoparticle quantity is partially compensated by aggregates with lower dipolar moments. This compensation can be added to the possible disaggregation process contribution, which is favorable to increase the order parameter. In such a situation, the resulting global effect leads to a weak concentration dependence of $\delta T_{N\text{-}I}$ and $\delta T_{\mathrm{Sm}A\text{-}N}$, which corresponds probably to $\phi_{\mathrm{NP}} = 0.27\%$ and 0.54% in Fig. 4(c).

(b) Figure 4(c) shows that for each concentration, $\delta T_{N\text{-}I}$ is higher than $\delta T_{\mathrm{Sm}A\text{-}N}$. This is linked to the lower viscosity of the liquid crystal at the nematic-isotropic phase transition [31]. Indeed, the low viscosity is favorable for the permanent dipole orientation under ac electric field.

IV. CONCLUSION

In this work, we showed that phase-transition temperatures obtained from dielectric measurements are higher than those determined by DSC characterization. This is due to the increase of the order parameter under the ac electric field used during the dielectric characterization. The increase of phase-transition temperatures is explained by two phenomena that can coexist when the electric field is sufficiently high: an amplification of the coupling between the single-dipole nanoparticles and the liquid-crystal order parameter, and a separation of nanoparticles in aggregates. These effects are stronger near the nematic-isotropic phase transition due to the lower liquid-crystal viscosity, which is favorable for nanoparticle orientation under electric field.

ACKNOWLEDGMENTS

We would like to thank Y. Reznikov and O. Grabar from the Institute of Physics (Kiev, Ukraine) for kindly providing the $Sn_2P_2S_6$ nanoparticles, and J. F. Blach from the Université d'Artois (Lens, France) for helpful discussions.

[1] Y. Reznikov, O. Buchnev, O. Tereshchenko, V. Reshetnyak, A. Glushchenko, and J. West, Appl. Phys. Lett. **82**, 1917 (2003).

[2] F. Li, J. West, A. Glushchenko, C. I. Cheon, and Y. Reznikov, J. Soc. Inf. Display **14**, 523 (2006).

[3] M. Kaczmarek, O. Buchnev, and I. Nandhakumar, Appl. Phys. Lett. **92**, 103307 (2008).

[4] A. Lorenz, N. Zimmermann, S. Kumar, D. R. Evans, G. Cook, and H.-S. Kitzerow, Phys. Rev. E **86**, 051704 (2012).

[5] M. V. Rasna, L. Cmok, D. R. Evans, A. Mertelj, and S. Dhara, Liq. Cryst. **42**, 1059 (2015).

[6] Y. Shiraishi, N. Toshima, K. Maeda, H. Yoshikawa, J. Xu, and S. Kobayashi, Appl. Phys. Lett. **81**, 2845 (2002).

[7] K. K. Vardanyan, D. M. Sita, R. D. Walton, W. M. Saidel, and K. M. Jones, RSC Adv. **3**, 259 (2013).

[8] I. Musevic, M. Skarabot, D. Babic, N. Osterman, I. Poberaj, V. Nazarenko, and A. Nych, Phys. Rev. Lett. **93**, 187801 (2004).

[9] K. Takizawa, K. Kodama, and K. Kishi, Appl. Opt. **37**, 3181 (1998).

[10] B. Splingart, N. Tentillier, F. Huret, and C. Legrand, Mol. Cryst. Liq. Cryst. **368**, 183 (2001).

[11] F. Dubois, F. Krasinski, B. Splingart, N. Tentillier, C. Legrand, A. Spodlo, and R. Dabrowski, Jpn. J. Appl. Phys. **47**, 3564 (2008).

[12] L. M. Lopatina and J. V. Selinger, Phys. Rev. E **84**, 041703 (2011).

[13] D. R. Evans, S. A. Basun, G. Cook, I. P. Pinkevych, and V. Y. Reshetnyak, Phys. Rev. B **84**, 174111 (2011).

[14] Y. Lin, R. Douali, F. Dubois, A. Segovia-Mera, and A. Daoudi, Eur. Phys. J. E **38**, 103 (2015).

[15] J. Jadzyn, L. Hellemans, G. Czechowski, C. Legrand, and R. Douali, Liq. Cryst. **27**, 613 (2000).
[16] A. Mertelj, L. Cmok, M. Copic, G. Cook, and D. R. Evans, Phys. Rev. E **85**, 021705 (2012).
[17] G. Cordoyiannis, L. K. Kurihara, L. J. Martinez-Miranda, C. Glorieux, and J. Thoen, Phys. Rev. E **79**, 011702 (2009).
[18] K. Denolf, G. Cordoyiannis, C. Glorieux, and J. Thoen, Phys. Rev. E **76**, 051702 (2007).
[19] M. V. Gorkunov and M. A. Osipov, Soft Matter **7**, 4348 (2011).
[20] A. Matsuyama and R. Hirashima, J. Chem. Phys. **128**, 044907 (2008).
[21] A. Matsuyama, J. Chem. Phys. **131**, 204904 (2009).
[22] M. A. Bouchiat and D. Langvin-Cruchon, Phys. Lett. A **34**, 331 (1971).
[23] M. Slavinec, G. D. Crawford, S. Kralj, and S. Zumer, J. Appl. Phys. **81**, 2153 (1997).
[24] A. Alexe-Ionescu, A. Th. Ionescu, E. S. Barna, N. Scaramuzza, and G. Strangi, J. Phys. Chem. B **107**, 5487 (2003).
[25] N. Scaramuzza, C. Berlic, E. S. Barna, G. Strangi, V. Barna, and A. Th. Ionescu, J. Phys. Chem. B **108**, 3207 (2004).
[26] M. Schadt, K. Schmitt, V. Kozinkov, and V. Chigrinov, Jpn. J. Appl. Phys. **31**, 2155 (1992).
[27] C. Bahr and G. Heppke, Phys. Rev. A **41**, 4335 (1990).
[28] R. Ranjini, M. V. Matham, and N. T. Nguyen, Appl. Opt. **53**, 2773 (2014).
[29] E. I. Rjumtsev, M. A. Osipov, T. A. Rotinyan, and N. P. Yevlampieva, Liq. Cryst. **18**, 87 (1995).
[30] W. Yan, S. Li, Y. Zhang, Q. Yao, and S. D. Tse, J. Phys. Chem. C **114**, 10755 (2010).
[31] S. DasGupta, P. Chattopadhyay, and S. K. Roy, Phys. Rev. E **63**, 041703 (2001).